Journal of Nuclear Materials 400 (2010) 56–63

Contents lists available at ScienceDirect

Journal of Nuclear Materials

journal homepage: www.elsevier.com/locate/jnucmat

Dislocation loop evolution under ion irradiation in austenitic stainless steels

A. Etienne [a,*], M. Hernández-Mayoral [b], C. Genevois [a], B. Radiguet [a], P. Pareige [a]

[a] Groupe de Physique des Matériaux, Université et INSA de Rouen, UMR CNRS 6634, BP 12, 76 801 Saint Etienne du Rouvray Cedex, France
[b] Division of Materials, CIEMAT, Avenida Complutense 22, 28040 Madrid, Spain

ARTICLE INFO

Article history:
Received 2 June 2009
Accepted 8 February 2010

ABSTRACT

A solution annealed 304 and a cold worked 316 austenitic stainless steels were irradiated from 0.36 to 5 dpa at 350 °C using 160 keV Fe ions. Irradiated microstructures were characterized by transmission electron microscopy (TEM). Observations after irradiation revealed the presence of a high number density of Frank loops. Size and number density of Frank loops have been measured. Results are in good agreement with those observed in the literature and show that ion irradiation is able to simulate dislocation loop microstructure obtained after neutron irradiation.

Experimental results and data from literature were compared with predictions from the cluster dynamic model, MFVIC (Mean Field Vacancy and Interstitial Clustering). It is able to reproduce dislocation loop population for neutron irradiation. Effects of dose rate and temperature on the loop number density are simulated by the model. Calculations for ion irradiations show that simulation results are consistent with experimental observations. However, results also show the model limitations due to the lack of accurate parameters.

© 2010 Elsevier B.V. All rights reserved.

1. Introduction

Fuel assemblies and control rods of pressurized water reactor (PWR) are held by internal structures. Theses structures are constituted of vertical baffles made of solution annealed 304 austenitic stainless steel (SA 304 SS) fixed to baffle radial support by a large number of bolts made of cold worked 316 austenitic stainless steel (CW 316 SS). These components, located close to the reactor core, undergo a large neutron flux at temperatures between 280 and 380 °C. This irradiation induces a loss of corrosion resistance and an increase of the yield stress [1]. The change of strength and ductility is mainly due to the accumulation of point defect clusters, mostly Frank loops (faulted dislocation loops with a Burger vector $a_0\langle 1\,1\,1\rangle$ in $\{1\,1\,1\}$ planes) which hold up the motion of dislocations [2–6]. This radiation - induced hardening may be an important contributory factor to stress corrosion sensitivity [7], and so may contribute, for example, to the cracking of baffle bolts in PWRs by irradiation assisted stress corrosion cracking (IASCC) [8–11].

Since the evolution of the macroscopic properties is related to the evolution of the microstructure, the understanding of its evolution under irradiation is essential to predict time-of-life of internals.

Multi-scale modelling (MSM) of material behaviour is a promising approach to predict time-of-life of components of nuclear power reactors [12,13] as it is developed, for example, in two European programs, Perfect [14] and Perform60 [15]. Of course, the use of a multi-scale model involves experimental validation, preferably at each scale, of all used models. Among different models used in MSM in this field of nuclear materials, cluster dynamic (CD) codes such as MFVIC (Mean Field Vacancy and Interstitial Clustering), developed by Hardouin Duparc [16], allow to simulate the evolution of point defect and point defect cluster populations under irradiation. This code was first adapted to austenitic steels by Pokor [17,18] and then by Garnier [19]. Thus, a direct comparison between simulation and experimental observations by TEM, at least for large defect sizes, might be done. In addition, CD is the only one modelling technique that can give long term prediction, main subject of PWR structural materials nowadays.

This paper, in addition to experimental irradiation, will describe how CD model is able to simulate dislocation loop population under ion irradiation. A scale to scale confrontation, between experimental and model results, brings fundamental understanding of basic mechanisms of irradiation damage when agreement occurs. The irradiation under ions is indeed important as one of the main technical obstacles to study and obtain experimental data on irradiation effects on specimens from internal structures is the high radioactivity that such steels may reach and the high costs for their characterization. The low number of experimental reactor is an additional difficulty [20]. This is the reason why, for several years, the development of the use of charged particle irradiations, like ion irradiations, has been pursued [20–24]. Ion irradiation is a way to produce displacement cascades with controlled parameters (temperature, dose rate, dose, etc.) and without inducing radioactivity

* Corresponding author. Tel.: +33 2 32 76 94 58; fax: +33 2 32 95 50 32.
E-mail address: auriane.etienne@etu.univ-rouen.fr (A. Etienne).

0022-3115/$ - see front matter © 2010 Elsevier B.V. All rights reserved.
doi:10.1016/j.jnucmat.2010.02.009

on materials. Thus, the use of model ion irradiations, with controlled irradiation conditions, is a way to test and validate models.

Even if these irradiations are not representative of neutron irradiation, in particular in terms of flux, ion irradiations can be used to understand fundamental effects of irradiation on materials. In this way, ion irradiation experiments have provided useful information to understand mechanisms of swelling, creep or segregation [25–30] in austenitic steels.

In this work, a SA 304 SS and a CW 316 SS were ion irradiated with 160 keV Fe^+ at different doses. These ions are used to understand effects of ballistic collisions as caused by a neutron spectrum in a PWR. Indeed, 160 keV Fe^+ ions correspond to the highest energy of primary knock-on atoms (PKA) generated by neutrons with energy of about 2 MeV. Thus, the point defect creation in the displacement cascade regime should be approximately reproduced. Ion irradiated samples were characterized by TEM in order to measure the size and number density of observed defects and to follow their evolution as a function of dose. Materials characteristics and experimental procedure are given in a first part. Results of the characterization of point defect clusters by TEM are presented in a second part.

These experimental results are compared with those obtained by cluster dynamic modelling using MFVIC in the last part.

2. Materials and experimental procedure

Materials investigated in this study are two 300 series SS commonly used for core internals of PWR namely a SA 304 SS and a CW 316 SS. Their chemical composition is given in Table 1.

Samples, for TEM studies, were prepared as disks of 3 mm in diameter. Thin foils were obtained by mechanical thinning of the disks down to 100 μm followed by electropolishing. Two different sets of samples were electropolished. The first was electropolished in a solution of 70% of ethanol, 20% of 2-butoxyethanol and 10% perchloric acid and the second with a solution of 5% perchloric acid in methanol.

Already prepared thin foils were irradiated with 160 keV Fe^+ ions in ion implantors IRMA at the Centre de Spectrométrie Nucléaire et de Spectrométrie de Masse (CSNSM – Orsay – France) [31] or at the University Complutense of Madrid [32]. The sample temperature was held at 350 °C and monitored using a thermocouple. The depth of penetration of iron ions with this energy is around 50 nm, that is to say the centre of the TEM thin foils (Fig. 1). The irradiation damage rate (in dpa s^{-1}), calculated with the software Stopping and Range in Ions in Matter (SRIM) [33] is quite homogeneous over the first 50 nm and then decreases to about one order of magnitude (in dpa s^{-1}) up to 100 nm in depth as shown in Fig. 1. It is estimated that, in the centre of the foils, the dose rates are 2.9×10^{-4} dpa s^{-1} for samples irradiated at CSNSM and 6.5×10^{-4} dpa s^{-1} for samples irradiated in Madrid. The dpa calculations are based on a displacement energy threshold of 40 eV and on the Kinchin–Pease formalism (quick calculation damage of SRIM). Irradiation conditions are summarized in Table 2.

Radiation - induced microstructure was characterized using TEM. The dislocation loops were examined using: (i) bright field (BF) images in two-beam conditions with reflection $g = 200$, (ii) weak beam dark field (WBDF) imaging, and (iii) the reciprocal lattice rod

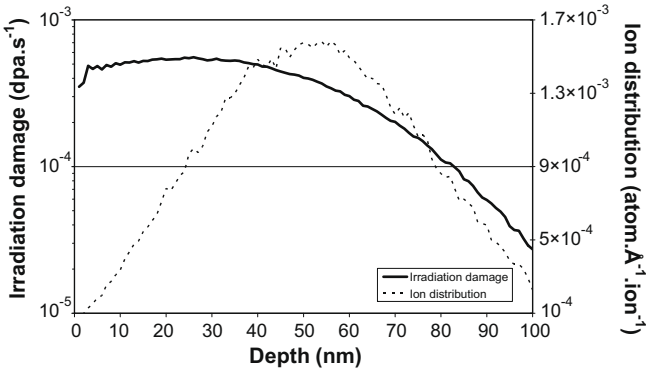

Fig. 1. Depth penetration of 160 keV Fe^+ ions and irradiation damage as a function of the depth, calculated with SRIM software.

(rel-rod) technique as described in Refs. [34,35]. The two first imaging techniques are used to obtain a general description of irradiated samples. The last one is used specifically to image Frank loops in order to measure their size and their number density.

A JEOL 2010 located at CIEMAT (Madrid, Spain) was used to perform BF and WBDF characterization for all specimens, and to perform the rel-rod technique for samples irradiated in Madrid. Frank loop characterization using the rel-rod technique for samples irradiated at CSNSM was performed on a JEOL 2010 located at the CEA-SRMA (Saclay, France), a FEI-Tecnai and a TOPCON 002B located in the CRISMAT laboratory (Caen, France). The main difference between these microscopes is the size of the contrast diaphragm (5 or 10 μm). The smaller the diaphragm is, the stronger the dark field contrast is. As it was shown by Gan and Was [23] it can result in some differences in measured dislocation loop density up to a factor 2. In each condition a maximum number of loops (between 50 to 970 loops) were imaged to obtain the average loop diameter and the number density. Only well defined Frank loop are measured that is to say that white spots which cannot be characterized are not taken into account. Indeed, as it can be seen in Figs. 3a and 4a, such white spots could be artefacts especially when larger contrast diaphragm is used. So, the mean diameter of loops could be slightly overestimated (thus a maximum mean diameter is obtained) and the density underestimated (thus a minimum loop number density is obtained). The given mean diameter is the average of visible loop diameters. The loop number density was obtained by multiplying by four the number of measured loops, as only one of the four families is imaged by the rel-rod technique and by considering 100 nm in thickness for all specimens. Results obtained in un-irradiated samples and in ion irradiated samples are presented in the following section.

3. Experimental results

Fig. 2a and c shows the microstructure of un-irradiated SA 304 and CW 316 respectively. The microstructure of SA 304 SS contains tangled dislocations and stacking faults. The un-irradiated CW 316 SS exhibits a microstructure composed of deformation bands, microtwins and a high number density of dislocations due to the

Table 1
Bulk composition of CW 316 and SA 304 SS (wt.%).

Alloy type	C	P	S	Si	Cr	Ni	Mn	Co	Mo	Cu
SA 304 SS	0.022	0.032	0.0007	0.36	18.61	9.86	1.79	0.06	–	0.25
CW 316 SS	0.054	0.027	0.022	0.68	16.60	10.60	1.12	0.12	2.25	0.24

Balance is iron.

Table 2
Irradiation conditions.

Dose (ions m^{-2})	Dose (dpa_{NRT})	Dose rate (ions m^{-2} s^{-1})	Dose rate (dpa s^{-1})	Implantor
2×10^{18}	0.36	3.5×10^{15}	6.5×10^{-4}	Madrid
5.6×10^{18}	1	1.56×10^{15}	2.9×10^{-4}	Irma CSNSM
7×10^{18}	1.25	3.5×10^{15}	6.5×10^{-4}	Madrid
2.6×10^{19}	5	1.56×10^{15}	2.9×10^{-4}	Irma CSNSM

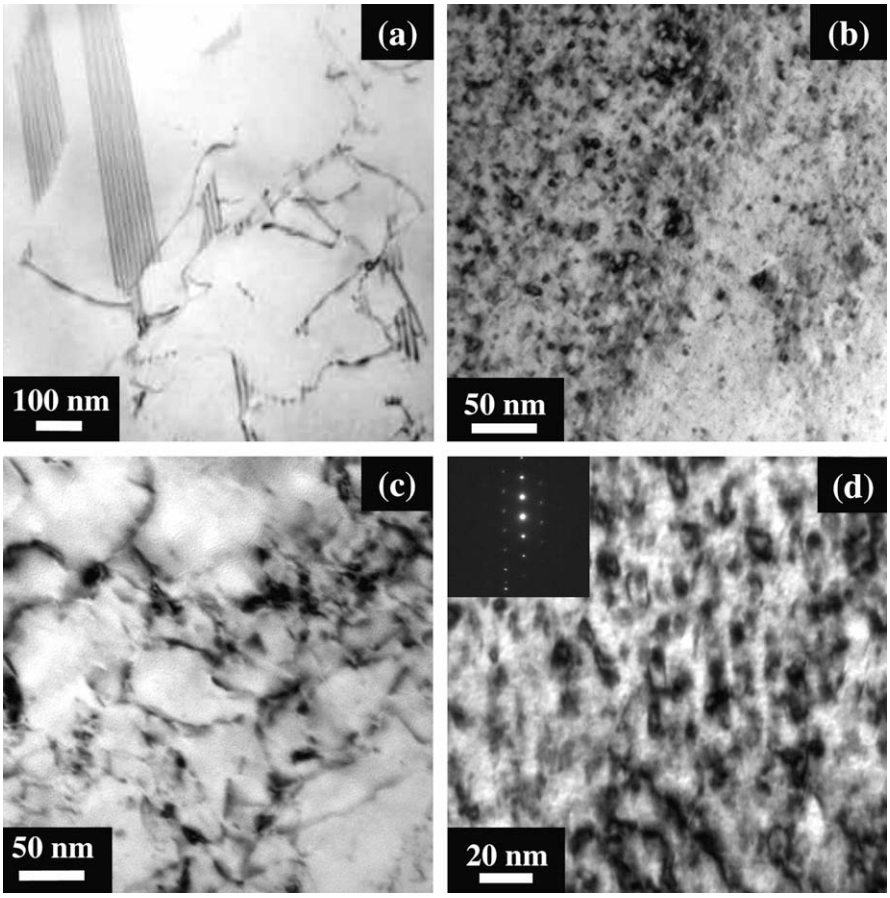

Fig. 2. Bright field TEM images of: (a) SA 304 SS un-irradiated, (b) SA 304 SS ion irradiated at 350 °C to 1 dpa, (c) CW 316 SS un-irradiated, and (d) ion irradiated at 350 °C at 1 dpa.

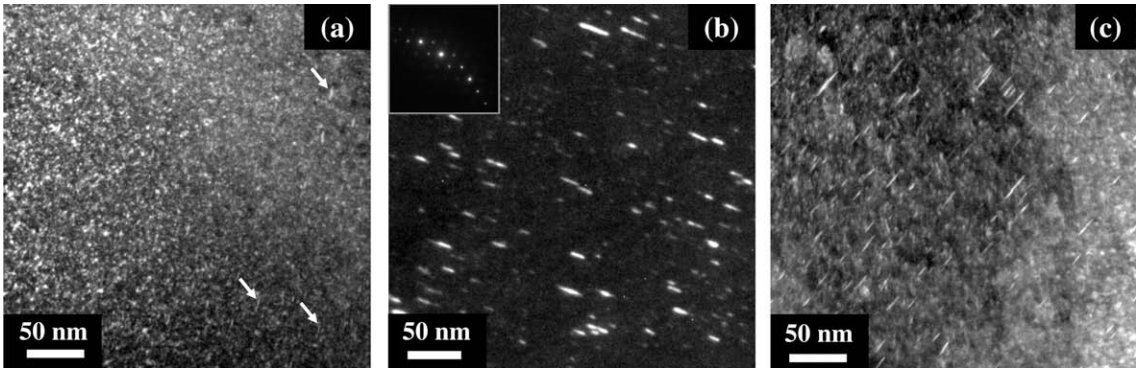

Fig. 3. Rel-rod dark field TEM images of the faulted Frank loops in SA 304 SS ion irradiated at 350 °C to (a) 1 dpa, (b) 1.25 dpa and (c) 5 dpa. The loop contrast is weak for the sample irradiated at 1 dpa. Only some loops, indicated with arrows, are visible.

cold work. A difference between un-irradiated samples and ion irradiated samples at 1 dpa (Fig. 2b and d) is clearly visible. After ion irradiation, black dots and dislocation loops are visible in both alloys. Rel-rod technique has been used in irradiated samples to image Frank loops and to measure their number density and diameters. Uncertainties on measurements are estimated to be

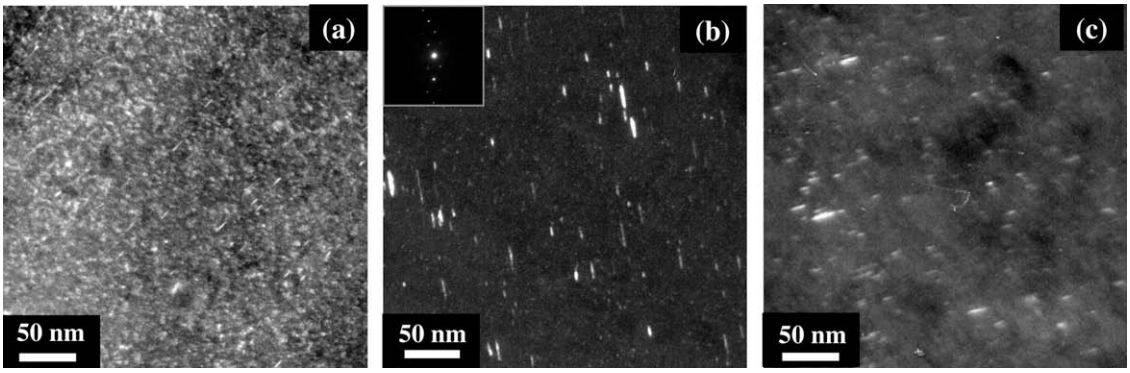

Fig. 4. Rel-rod dark field TEM images of the faulted Frank loops in CW 316 SS ion irradiated at 350 °C to (a) 1 dpa, (b) 1.25 dpa and (c) 5 dpa.

approximately 1 nm on the loop diameter. For loop number density, uncertainties come from the thickness of the thin foils by a factor 2 and from the imaging conditions (size of the contrast diaphragm) by a factor 2. So the dislocation number density ρ is between $\frac{\rho}{4}$ (maximum thickness and minimum number of loops) and 4ρ (minimum thickness and maximal number of loops).

Rel-rod images of the faulted Frank dislocation loops in SA 304 SS irradiated at 1, 1.25 and 5 dpa are shown in Fig. 3. The Frank loop contrast observed for the sample irradiated at 1 dpa is weak due to the size of the contrast diaphragm (10 μm in diameter). So dislocation density and dislocation size could not have been measured for this sample. Size distribution of Frank loops for SA 304 at doses of 1.25 and 5 dpa is depicted in Fig. 5. Imaging of Frank loops by the rel-rod technique in CW 316 SS irradiated at 1, 1.25 and 5 dpa are represented in Fig. 4. The size distribution of loops (from rel-rod images) was measured for each condition in which the number of loops is sufficient (>150). Loop size distribution for CW 316 irradiated at doses of 1, 1.25 and 5 dpa is also shown in Fig. 5. Loop size distributions are similar at 1.25 and 5 dpa for both SA 304 and CW 316. For irradiated sample at 1 dpa, the loop size distribution is narrower and shifted towards smaller sizes. The mean loop diameter and the maximum size of loops for each irradiation condition are given in Table 3. The mean diameter is about 5 nm at 1 dpa and increases with the dose and saturate at about 8 nm after 1.25 dpa.

Dislocation loop number densities measured from rel-rod images are given in Table 3 and represented as a function of dose in Fig. 7a. Loop number density is in the same order of magnitude for SA 304 and CW 316. As the loop diameter, the number density seems to increase up to 1 dpa and saturate for higher doses.

Fig. 6a shows the comparison between data from literature [18,22,36–41] and experimental results obtained in this study concerning the number density of dislocation loops. Results are in excellent agreement with the literature, especially for neutron irradiations at a temperature between 300 and 370 °C. Mean loop diameters between data from literature and results from this study are shown in Fig. 6b and can be compared. Mean loop diameter are between 4 and 10 nm when irradiation dose is lower than 1–3 dpa. The loop diameter increases with the dose and saturate after 5–10 dpa between 6 and 12 nm. It must also be noted that no difference between CW 316 and SA 304 SS is observed.

Table 3
Dislocation loop number density, mean loop diameter and maximum size of loops for ion irradiated SA 304 and CW 316 samples. Uncertainties are 1 nm for loop diameters and a factor 4 for loop number densities.

Material	Dose (dpa)	Loop number density (m^{-3})	Mean loop diameter (nm)	Maximum size of loops (nm)
SA 304	1.25	3×10^{22}	9.6	28.4
	5	4.1×10^{22}	8.1	27.5
CW 316	0.36	8×10^{21}	n.m.	n.m.
	1	2.8×10^{22}	5.3	18.8
	1.25	2.3×10^{22}	8.7	32.6
	5	2.8×10^{22}	8.3	31.4

n.m.: not measured.

Thus, in terms of dislocation loop density and size, the microstructure of Fe^+ irradiated samples are comparable to the one of samples irradiated with neutrons in experimental reactors [18,35,36,38,39], with neutrons in PWR conditions [36,37] or with protons [40,41]. Also, results obtained on Fe^+ irradiated samples are coherent with those obtained by Pokor et al. [22] on SA 304 and CW 316 irradiated with Ni^+ at 350 °C.

Fe^+ irradiations are able to reproduce dislocation loop microstructure observed in neutron irradiated samples.

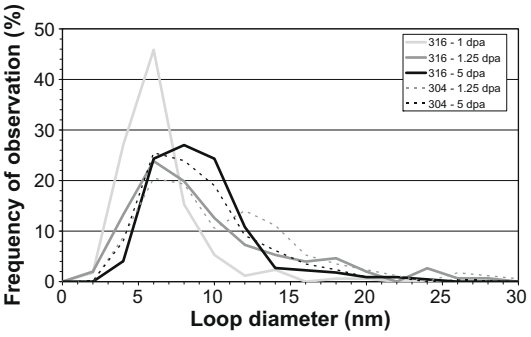

Fig. 5. Loop size distribution for SA 304 samples irradiated at 1.25 and 5 dpa and for CW 316 samples irradiated at 1, 1.25 and 5 dpa.

4. Cluster dynamic modelling

In this section, the ability of the CD model, MFVIC [16–19] to reproduce experimental results for different irradiation conditions, in particular Fe^+ irradiations, is examined. This model is described in detail in [17–19]. It predicts the evolution of point defect and point defect cluster populations under irradiation. The actual environment is replaced by a continuous medium in which point defect clusters are characterized by their size n and their type θ (interstitial or vacancy). The evolution of point defect cluster concentration as a function of time is given by reaction rate theory equations.

In this work, interstitial clusters are considered as 2D defects (dislocation loops) and vacancy clusters as 3D clusters (cavities). Only results concerning dislocation loops are taken into account as cavities were not studied in ion irradiated samples. Perfect loops are not studied neither, as some studies show that the majority of

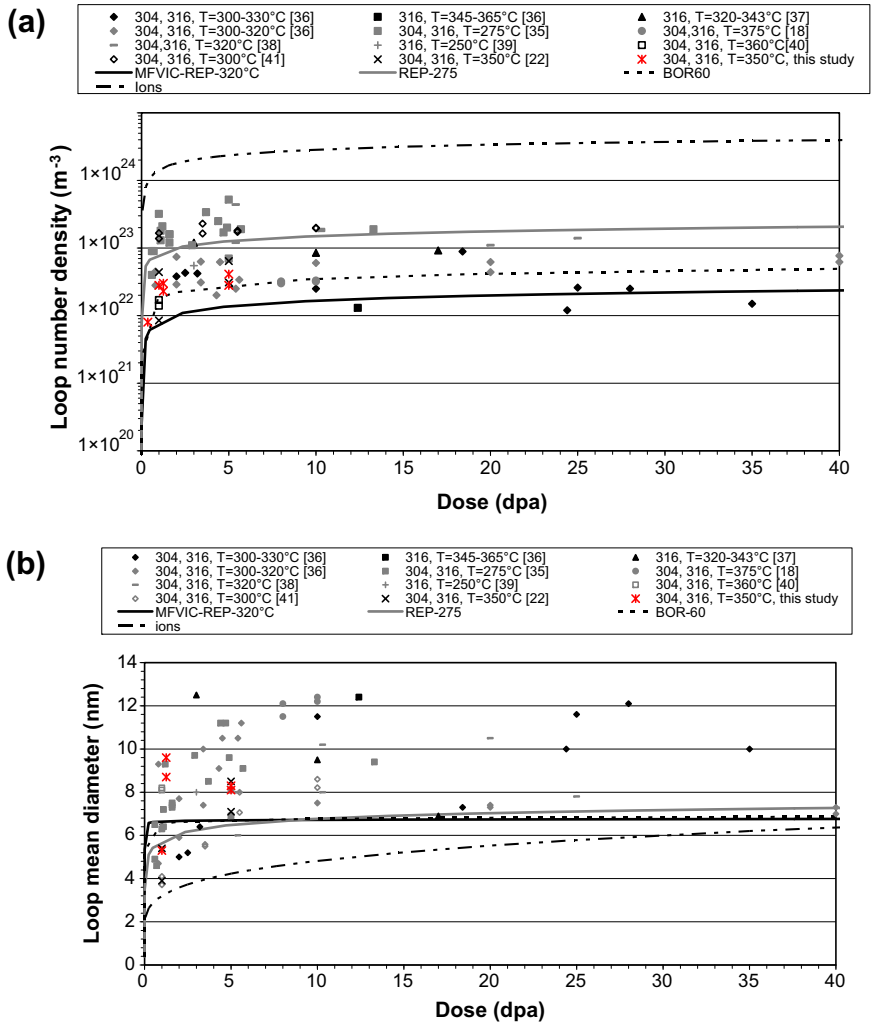

Fig. 6. (a) Loop number densities and (b) loop diameters measured for ion irradiated samples in this study and results obtained in the literature for neutron or proton irradiations [18,22,36–41] are compared to results from cluster dynamic calculations. Full black symbols are for neutron irradiations in PWR, full grey symbols for neutron irradiations in experimental reactors and open symbols for proton irradiations. Black and red crosses are for ion irradiations. Lines correspond to model results: BOR-60 (- - -), REP (—) and ions (– - - -)(For interpretation of the references to colour in this figure legend, the reader is referred to the web version of this article.).

dislocation loops in irradiated austenitic steels are faulted loops [17,35]. In addition, while some authors consider that Frank loops can be either interstitial or vacancy [35], in this work, Frank loops are supposed to be only interstitial [42,43]. Samples are considered as thin foils of 100 nm in thickness. Only mono-interstitials and mono-vacancies are supposed to be mobile.

As described in [18] two sets of parameters are required. The first set consists in material parameters. For this work, material parameters adjusted from [18] and available in [19] were used. They are listed in Table 4.

The second set of parameters is irradiation parameters. These parameters characterize the irradiation conditions: the dose rate (in $dpa_{NRT}\ s^{-1}$) and the displacement cascades (the fraction of surviving point defects compared to dpa_{NRT} and the fraction of these point defects directly agglomerated in the displacement cascade). They have been suggested by Pokor [17] for different experimental neutron irradiation conditions in a fast breeder reactor (BOR-60) and in a reactor presenting a mixed neutron spectrum (OSIRIS) for same materials as in this study. These irradiation parameters are listed in Table 5.

First, using these irradiation parameters, simulation results are compared with experimental measurements found in the literature (see Fig. 6). From these results it appears that the lower the irradiation temperature, the higher is the number density of dislocation loops observed. No trend is observed for loop diameter. The effect of dose rate is visible between irradiation in PWR (where the dose rate is about 9.10^{-8} dpa s^{-1}) and irradiations in experimental reactor like BOR-60 (where the dose rate is about 9.10^{-7} dpa s^{-1}). The higher the flux, the higher is the number density and the smaller is the loop diameter.

Several calculations have been performed. The first calculation was performed for a CW 316 SS neutron irradiated in BOR-60. The second concerns REP at 320 °C and 275 °C. Except the flux, the neutron spectrum is approximately the same in a mixed neutron reactor as in a PWR reactor [17]. So, irradiation parameters are considered the same for irradiations performed in OSIRIS than for irradiations performed in a PWR reactor (except the flux). Results are depicted in Fig. 6. As it can be seen in Fig. 6a CD modelling results, for loop number density, are in good agreement with results from the literature. The effect of dose rate is visible by comparing results for BOR-60 and REP at 320 °C. The trend observed in experimental results is the same for simulation results. Temperature effect is also simulated by the model, loop number density is higher for simulation at 275 °C than for simulation at 320 °C.

Fig. 6b represents the loop diameter as a function of dose. Results show that calculation reproduces the saturation of loop

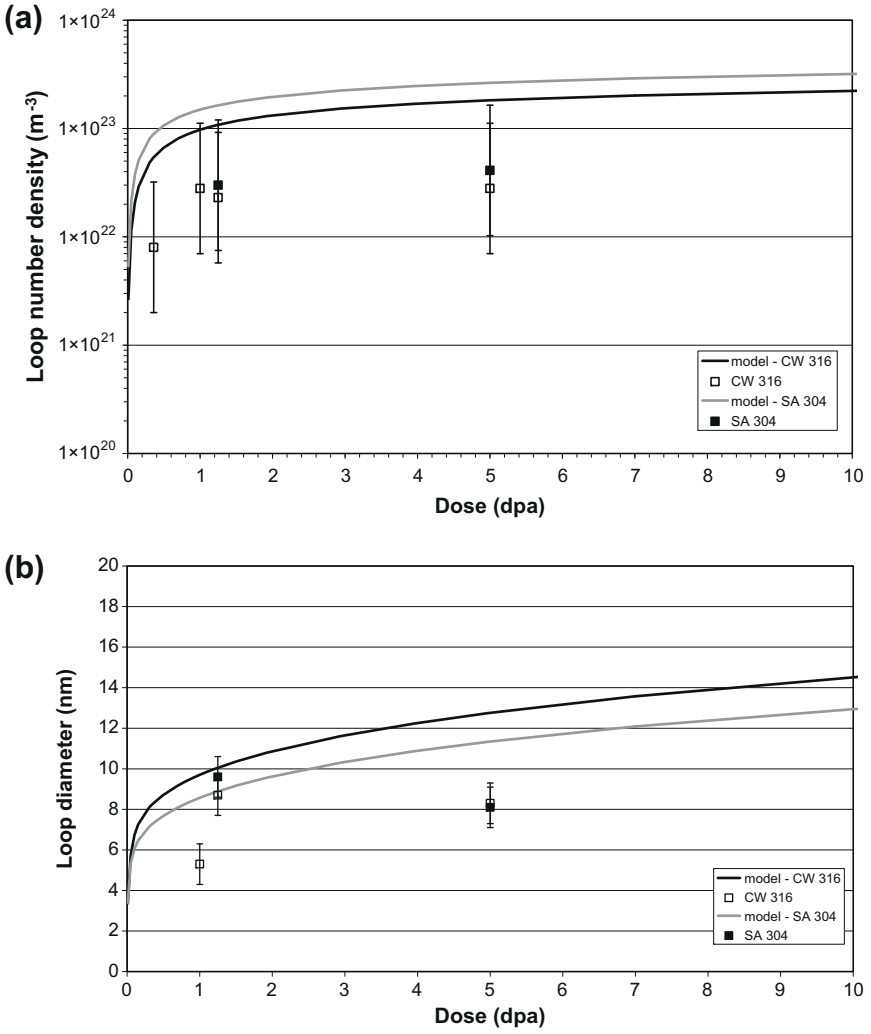

Fig. 7. Comparison of the calculated loop number density (a) and loop diameter (b) as a function of dose with experimental results for ion irradiated SA 304 and CW 316 in this study.

Table 4
Material parameters determined in [reference] for CW 316 and SA 304 SS.

Parameters	SA 304	CW 316
Interstitial migration energy	0.45 eV	0.43 eV
Vacancy migration energy	1.35 eV	1.35 eV
Pre-exponential factor for interstitial diffusivity	10^{-3} cm^2 s^{-1}	10^{-3} cm^2 s^{-1}
Pre-exponential factor for vacancy diffusivity	0.6 cm^2 s^{-1}	0.6 cm^2 s^{-1}
Interstitial formation energy	4.1 eV	4.1 eV
Vacancy formation energy	1.7 eV	1.7 eV
Di-interstitial binding energy	0.61 eV	0.61 eV
Di-vacancy binding energy	0.39 eV	0.39 eV
Recombination radius	0.7 nm	0.7 nm
Capture efficiency of interstitials by dislocations	1.1	1.1
Capture efficiency of vacancies by dislocations	1	1
Dislocation density	10^{10} m^{-2}	10^{14} m^{-2}
Thickness of the thin foil	100 nm	100 nm

Table 5
Irradiation parameters for neutron irradiations in a fast breeder reactor (BOR-60) and in a reactor presenting a mixed neutron spectrum (OSIRIS). Irradiation parameters are also reported for Fe^+ ion irradiation. $f_i(n)$ and $f_v(n)$ are, respectively, the fraction of interstitials and vacancies clustering in the form of n-interstitials and n-vacancies in the displacement cascade.

Parameters	BOR-60	OSIRIS	Fe^+ ions
Cascade efficiency	0.15	0.30	0.30
$f_i(2)$	0.50	0.50	0.50
$f_i(3)$	0.20	0.20	0.02
$f_i(4)$	0.05	0.05	0
$f_v(2)$	0.10	0.05	0.05
$f_v(3)$	0.70	0.02	0.02
$f_v(4)$	0.10	0.02	0.02

diameter but slightly underestimates the loop diameter. Dose rate and temperature effects are not clearly visible. Calculations, not represented here for clarity, were also performed for SA 304 SS. Results are in excellent agreement with results from literature and show some differences between CW 316 and SA 304. Loop diameter for SA 304 SS is higher than for CW 316 SS and does not saturate so rapidly. Although, no difference is visible for experimental data, this difference can be explained by the high number density of dislocations introduced by cold working in CW 316 SS.

The model is able to reproduce loop population trends for different neutron irradiation conditions. As depicted in Fig. 6a and b, simulation results obtained at 320 °C and 275 °C show that the model can reproduce the temperature effect on dislocation loop population. Also, simulation results for irradiations in BOR-60 and in a PWR show that the model can emulate dose rate effects.

Using the same parameters, a second set of simulations is performed, this time, for Fe^+ ion irradiations. For calculations, a dose rate of 2.9×10^{-4} dpa s^{-1}, an irradiation temperature of 350 °C and OSIRIS irradiation parameters were used. Note that, although ion irradiations were performed at two different dose rates, the difference in dose rate for both Fe^+ irradiations is small enough to neglect it in calculations. Comparison between model and experimental results for number density and loop diameter are depicted in Fig. 6a and b. The calculated loop density is about two orders of magnitude higher than the experimental data. The calculated loop diameter is not in agreement with experimental data either. It is underestimated by about 50% in comparison with experimental results. These discrepancies cannot be attributed to measurement uncertainties.

As materials (SA 304 and CW 316) are the same as used for neutron calibration of the model by Pokor, observed differences are, a priori, not due to material parameters but they can be attributed to irradiation parameters and more particularly to the cascade parameters. The aim is to adjust irradiation parameters to obtain a good agreement between experimental results and simulation results.

The cascade efficiency (per NRT displacement) η for 160 keV Fe^+ is considered equal to 0.30 [44–46]. The in-cascade interstitial and vacancy clustering are adjustable parameters. Parameters have been adjusted in order to have a good compromise between experimental and calculated data for loop number density and loop size. The best set of irradiation parameters is listed in Table 5. The fraction of in-cascade interstitial clusters is about 50%, which is consistent with results from Molecular Dynamics (MD) for neutron irradiations [46,47], clusters are essentially in the form of di-interstitials. The fraction of in-cascade vacancy cluster is about 9%, consistent with the one found by Gan et al. [48] for proton irradiations.

The results of the calculations of loop density and loop size, using the adjusted irradiation parameters for ion irradiation, are given in Fig. 7. Fig. 7a shows that the loop density obtained by the model is consistent with the one measured experimentally. At the same time, there is a slight discrepancy between loop diameter estimated by cluster dynamics and loop diameter observed by TEM (Fig. 7b). Experimentally, the loop diameter seems to saturate with the dose, whereas the simulation results do not show saturation. In addition, the model overestimates the loop diameter.

Simulation results are in good agreement with experimental results for neutron irradiations. Actually, all parameters (irradiation and material parameters) have been adjusted for neutron irradiations. By changing only irradiation parameters, simulation results are consistent with experimental results obtained on Fe^+ irradiated thin foils but the agreement between both sets of data is not excellent. As the only difference between neutron irradiation and ion irradiation is irradiation parameters this fact suggests that the material parameters are not optimal. So, material parameters should be improved in order to simulate with an excellent agreement experimental data. To refine material parameters, ab-inito calculations, as for example, point defect binding energy and point defect migration energy, are needed. Also, it seems useful to introduce mobility for small point defect clusters. Indeed, some papers in the literature show that small clusters are mobile [48–52]. Ab-inito calculations could bring useful information that could quantify mobilities for small point defect clusters.

Furthermore, irradiation parameters should also be more accurate, especially for ion irradiation. In this case, results from MD in term of in-cascade clustering could be very useful. Indeed, MD results present in the literature are mainly obtained for neutron irradiation in pure metals [47,53]. Results for ion irradiations in Fe–Cr–Ni obtained by MD seem essential for improving this model.

5. Conclusion

A SA 304 and CW 316 SS have been ion irradiated at different doses in order to characterize dislocation loop population by TEM. Results show a high number density of Frank loops that increases with the dose and saturates after 1.25 dpa. A similar trend is observed for the loop diameter. Results are in good agreement with what is reported in the literature, showing that ion irradiations are able to reproduce loop evolution under irradiation.

Simulation results are in good agreement with experimental observations for neutron irradiations. Effects of dose rate and temperature are reproduced by the model.

As the only difference between neutron and ion irradiations is the irradiation conditions, cascade parameters have been adjusted for ion irradiations. Results between calculations and observations are consistent but the agreement is not excellent.

Material and irradiation parameters of this CD model should be improved in order to reproduce experimental data. Small cluster mobility should be taken into account. That implies that mobility data for Fe–Cr–Ni are needed. Finally, some DM calculations about displacement cascades in Fe–Cr–Ni can produce some essential data that further improve the agreement between model and experimental results.

Acknowledgements

This work is a part of the research program of the EDF-CNRS joint laboratory EM^2VM (Study and Modelling of the Microstructure for Ageing of Materials). The authors are grateful to Odile Kaitasov for performing ion irradiation at the CSNSM laboratory at Orsay (France) and to Pablo Fernández for performing the ion irradiation at the University Complutense of Madrid (Spain). We gratefully acknowledge Denis Pelloquin from CRISMAT at Caen (France) for providing time on the electron microscope. The authors would like to thank Alexandra Renault and Jérôme Garnier (CEA-SRMA, Saclay) for helpful and fruitful discussions about rel-rod technique and MFVIC.

References

[1] G.E. Lucas, J. Nucl. Mater. 206 (1993) 287–305.
[2] M.L. Grossbeck, P.J. Maziasz, A.J. Rowcliffe, J. Nucl. Mater. 191 (1992) 808.
[3] G.R. Odette, D. Frey, J. Nucl. Mater. 85 (1979) 817.
[4] F. Garner, M.L. Hamilton, N.F. Panayotou, G.D. Johnson, J. Nucl. Mater. 103 (1981) 803.
[5] N. Yoshida, H.L. Heinisch, T. Muroga, K. Araki, M. Kiritani, J. Nucl. Mater. 179 (1991) 1078.
[6] P.B. Hirsch, Point Defect Cluster Hardening, in: R.E. Smallman, J.E. Harris (Ed.), Vacancies, vol. 76, 1976.
[7] P. Scott, J. Nucl. Mater. 211 (1994) 101.
[8] R. Cauvin, O. Goltrant, Y. Rouillon, E. Verzaux, A. Cazus, P. Dubuission, P. Poitrenaud, S. Bellet, in: Proceedings of the International Symposium Fontevraud III, Société Française d'Energie Nucléaire, 1994, pp. 54–65.
[9] G. Pironet, A. Heuzé, O. Goltrant, R. Cauvin, in: Proceedings of the International Symposium Fontevraud IV, Société Française d'Energie Nucléaire, 1998, pp. 195–2006.
[10] O. Goltrant, R. Cauvin, D. Deydier, A. Trenty, in: Proceedings of the International Symposium Fontevraud III, Société Française d'Energie Nucléaire, 1998, pp. 183–193.
[11] I. Monnet, G.M. Decroix, P. Dubuisson, J. Reuchet, O. Morlent, in: Proceedings of the International Symposium Fontevraud IV, Société Française d'Energie Nucléaire, 2002, pp. 371–379.
[12] M. Samaras, M. Victoria, W. Hoffelner, J. Nucl. Mater. (2009), doi:10.1016/j.jnucmat.2009.03.016.
[13] A. Barbu, C.R. Phys. 9 (2008) 353–361.
[14] Web Site European Program, <http://fp6perfect.net/site/index.htm>.
[15] European Program Perform60, <http://cordis.europa.eu>.
[16] A. Hardouin Duparc, C. Moingeon, N. Smetniansky-de-Grande, A. Barbu, J. Nucl. Mater. 302 (2002) 143–155.
[17] C. Pokor, Institut National Polytechnique de Grenoble, PhD Thesis, 2003.
[18] C. Pokor, Y. Brechet, P. Dubuisson, J.-P. Massoud, A. Barbu, J. Nucl. Mater. 326 (2004) 19–29.
[19] J. Garnier, Institut National Polytechnique de Grenoble, PhD Thesis, 2007.

[20] G. Was, J. Busby, T. Allen, E. Kenik, A. Jenssen, S. Bruemmer, J. Gan, A. Edwards, P. Scott, P. Andresen, J. Nucl. Mater. 300 (2002) 198–216.
[21] R. Krummeich, P. Pareige, J.-P. Massoud, S. Jumel, Surf. Interf. Anal. 36 (2004) 575–580.
[22] C. Pokor, J-P. Massoud, P. Pareige, J. Garnier, D. Loisnard, P. Dubuisson, B. Doisneau, Y. Brechet, in: 12th International Conference on Environmental Degradation of Materials in Nuclear Systems – Water Reactors. The Minerals, Metals and Materials Society, Salt Lake City, 2005.
[23] J. Gan, G.S. Was, J. Nucl. Mater. 297 (2001) 161–175.
[24] N. Sakaguchi, H. Kinoshita, S. Watanabe, Y. Sueishi, N. Akasaka, H. Takahashi, J. Nucl. Mater. 382 (2008) 197–202.
[25] L.K. Mansur, J. Nucl. Mater. 216 (1994) 97–123.
[26] L.K. Mansur, M.H. Yoo, J. Nucl. Mater. 85–86 (1979) 523–532.
[27] F. Garner, J. Nucl. Mater. 117 (1983) 177.
[28] R.A. Johnson, N.Q. Lam, J. Nucl. Mater. 69–70 (1978) 424.
[29] N.Q. Lam, A. Kumar, H. Wiedersich, in: H.R. Brager. J.S. Perrin (Eds.), Effects of Radiation on Materials: 11th Conference, ASTM STP 782, American Society for Testing Materials, West Conshohocken, PA, 1982, pp. 985.
[30] L.E. Rehn, P.R. Okamoto, Phase Transformations During Irradiation, in: F.V. Nolfi (Ed.), Applied Science, New York, 1983, p. 247.
[31] J. Chaumont, F. Lalu, M. Salomé, Nucl. Instr. Method 189 (1981) 193.
[32] J.M. Martin, G. González-Díaz, Nucl. Instr. Method B 88 (1994) 331.
[33] J.F. Ziegler, J.P. Biersack, U. Littmark, The Stopping and Range of Ions in Matter, Pergamon Press, New York, 1985.
[34] D.J. Edwards, E.P. Simonen, S.M. Bruemmer, Microsctructural processes in irradiated materials, in: G.E. Lucas, L.L. Snead, M.A. Kirk, R.G. Elliman (Eds.), Materials Research Society Symposium, vol. 650, 2000, pp. R2.7.
[35] D.J. Edwards, E.P. Simonen, S.M. Bruemmer, J. Nucl. Mater. 317 (2003) 13–31.
[36] C. Pokor, Y. Thebault, J.P. Massoud, M. Delnondedieu, D. Loisnard, P. Dubuisson, J. Kocik, E. Keilova, E. Lemaire, N. Ligneau, Fontevraud 6: Contribution of Materials Investigations to Improve the Safety and Performance of LWRs, 2006.
[37] D. Edwards, F. Garner, E. Simonen, S. Bruemmer, Characterization of Neutron-Irradiated 300-Series Stainless Steels to Assess Mechanisms of Irradiation-Assisted Stress Corrosion Cracking: Volume 2: Core Components, EPRI, Palo Alto, CA, 2001. pp. 1001497.
[38] D.J. Edwards, A. Schemer-Kohrn, S. Bruemmer, Characterization of Neutron-Irradiated 300-series Stainless Steels, EPRI, Palo Alto, CA, 2006. pp. 2009896.
[39] N. Hashimoto, E. Wakai, J.P. Robertson, J. Nucl. Mater. 273 (1999) 95.
[40] G.S. Was, T.R. Allen, J.T. Busby, J. Gan, D. Damcott, D. Carter, M. Atzmon, E.A. Kenik, J. Nucl. Mater. 270 (1999) 96.
[41] B.H. Sencer, G.S. Was, M. Sagisaka, Y. Isobe, G.M. Bond, F.A. Garner, J. Nucl. Mater. 323 (2003) 18.
[42] M. Suzuki, A. Sato, N. Nagakawa, H. Shiraishi, Philos. Mag. A 65 (1992) 1309.
[43] L. Boulanger, F. Soisson, Y. Serruys, J. Nucl. Mater. 233–237 (1996) 1004.
[44] B. Radiguet, A. Barbu, P. Pareige, J. Nucl. Mater. 306 (2007) 104–117.
[45] D.J. Bacon, A.F. Calder, F. Gao, J. Nucl. Mater. 251 (1997) 1–12.
[46] C. Domain, J. Ruste, C.S. Becquart, Etude par simulation numérique du dommage d'irradiation: Application au fer pur et aux alliages fer-cuivre, Rapport EdF HT-41/97/010/B, 1998.
[47] R.E. Stoller, L.R. Greenwood, J. Nucl. Mater. 271–272 (1999) 57.
[48] J. Gan, G.S. Was, R.E. Stoller, J. Nucl. Mater. 299 (2001) 53–67.
[49] N.V. Doan, R. Vascon, Nucl. Instrum. Meth. Phys. Res. B: Beam Interact. Mater. Atoms 135 (1998) 207.
[50] N.V. Doan, J. Nucl. Mater. 283–287 (2000) 763.
[51] V.A. Borodin, A.I. Ryazanov, J. Nucl. Mater. 256 (1998) 47.
[52] M. Kiritani, J. Nucl. Mater. 251 (1997) 237.
[53] R. Stoller, J. Nucl. Mater. 276 (2000) 22.